

What the Gribov copy tells on the confinement and the theory of dynamical chiral symmetry breaking

Sadataka Furui*

School of Science and Engineering, Teikyo University, 320-8551 Japan.

Hideo Nakajima†

Department of Information Science, Utsunomiya University, 321-8585 Japan.

(Dated: December 2, 2024)

We performed lattice Landau gauge QCD simulation on $\beta = 6.0, 16^4, 24^4, 32^4$ and $\beta = 6.4, 32^4, 48^4$ and 56^4 by adopting the gauge fixing that minimizes the norm of the gauge field, and measured the running coupling by using the gluon propagator and the ghost propagator. In view of ambiguity in the vertex renormalization factor \tilde{Z}_1 in the lattice, we adjust the normalization of the running coupling by the perturbative QCD results near the highest momentum point. It has a maximum $\alpha_s(q) \simeq 2.0(3)$ at around $q = 0.5$ GeV and decreases as q approaches 0, and the Kugo-Ojima parameter reached $-0.83(2)$. The infrared exponent of the ghost propagator at 0.4GeV region is $\alpha_G = 0.20$ but there is an exceptional configuration with $\alpha_G = 0.27$. The features of the exceptional configuration are investigated by measuring one-dimensional Fourier transform(1-d FT) of the gluon propagator transverse to 4 lattice axes. We observe that the 1-d FT along a specific axis of the exceptional configuration violates reflection positivity and the average of the Cartan subalgebra components of the Kugo-Ojima parameter along this axis is consistent to -1. The exceptional configuration is compatible with the infrared fixed point $\alpha_s(0) \sim 2.5(5)$ and $\kappa = 0.5$ suggested by the Dyson-Schwinger approach in the multiplicative renormalizable scheme.

PACS numbers: 12.38.Gc, 11.15.Ha, 11.15.Tk

I. INTRODUCTION

The lattice Landau gauge QCD simulation suffers from Gribov copy problem and its effect on the confinement was discussed by several authors [1, 2, 3, 4]. As a method for obtaining the unique gauge, we adopted the fundamental modular gauge (FMG) i.e. a configuration with the minimum norm of the gauge field and studied the Gribov copy problem in $SU(2)$ [5]. We compared the absolute minimum configuration obtained by the parallel tempering method and the 1st copy which is obtained by the random gauge transformation. We observed that the FMG configurations and the 1st copy which is in the Gribov region but not necessarily in the FM region have the following differences: 1) The absolute value of the Kugo-Ojima parameter c [6, 7], which gives the sufficient condition of the confinement, of the FMG is smaller than that of the 1st copy. 2) The singularity of the ghost propagator of the FMG is less than that of the 1st copy. 3) The gluon propagator of the two copies are almost the same within statistical errors. 4) The horizon function deviation parameter h of the FMG is not closer to 0, i.e. the value expected in the continuum limit, than that of the 1st copy.

The proximity of the FM region and the boundary of the Gribov region in $SU(2)$ in $8^4, 12^4$ and 16^4 lattices with

$\beta = 0, 0.8, 1.6$ and 2.7 was studied in [8]. The tendency that the smallest eigenvalue of the Faddev-Popov matrix of the FMG and that of the 1st copy come closer as β and lattice size become larger was observed, although as remarked in [8] the physical volume of $\beta = 2.7, 16^4$ lattice is small and not close to the continuum limit. Qualitative features of the profile of the Morse function

$$\mathcal{E}[g] = \frac{1}{2} \sum_{\mu,a} \int d^4x \{[A_\mu^{(g)}]^a(x)\}^2 \quad (1)$$

where $g = e^{\epsilon \cdot \lambda}$, was sketched as a function with respect to the magnitude of the infinitesimal gauge transformation parameter ϵ and a parameter r which is defined by 2nd, 3rd and 4th derivative of $\mathcal{E}[g]$ with respect to ϵ at the origin. The simulation suggests that as the β and lattice size become large, the parameter r decreases. The meaning of the parameter r is such that larger r than the critical value implies an existence of a smaller local minimum than that of the origin.

The difference of the 1st copy and the FMG in the $\beta = 2.2, 16^4$ lattice [5] indicates that the FMG does not overlap with the boundary of the Gribov region in that simulation. In the Langevin formulation of QCD, Zwanziger conjectures that the path integral over the FM region will become equivalent to that over the Gribov region in the continuum [3]. This conjecture is consistent with the view that the boundary of the FMG and that of the Gribov region overlaps and the probability distribution is accumulated in this overlapped region. On the lattice, when β and the lattice size is not large enough, distribution of Gribov copies i.e. statistical weight of the copies is crucial for extracting sample averages.

*Electronic address: furui@umb.teikyo-u.ac.jp; URL: http://albert.umb.teikyo-u.ac.jp/furui_lab/furuipbs.htm

†Electronic address: nakajima@is.utsunomiya-u.ac.jp

In the previous paper [7], we measured the QCD running coupling and the Kugo-Ojima parameter in $\beta = 6.0, 16^4, 24^4, 32^4$ and $\beta = 6.4, 32^4$ and 48^4 . The running coupling was found maximum of about 1.1 at around $q = 0.5$ GeV, and behaved either approaching constant or even decreasing as q approaches zero, and the Kugo-Ojima parameter was getting larger but staying around -0.8 in contrast to the expected value -1 in the continuum theory. Thus it is necessary to perform a larger lattice simulation and to study the dependence of the Gribov copy. We encountered a rather exceptional Gribov copy in $\beta = 6.4, 56^4$ which is close to the Gribov boundary and we consider it worthwhile to investigate that sample in some details. We analyse those data by comparing with continuum theory like Dyson-Schwinger equation(DSE).

There are extensive reviews on DSE for the Yang Mills theory [9, 10, 11]. The solution of DSE depends on ansatz of momentum truncation and what kind of loop diagrams are included. Two decades ago Mandelstam [12] projected the DSE for the gluon propagator by $\mathcal{P}_{\mu\nu}(q) = \delta_{\mu\nu} - q_\mu q_\nu/q^2$ and without including ghosts, assumed the gluon wavefunction renormalization factor in the form

$$Z(q^2) = \frac{b}{q^2} + C(q^2) \quad b = \text{const.} \quad (2)$$

Later Brown and Pennington [13] argued that in order to decouple divergent tadpole contribution, it is more appropriate to project the gluon propagator by $\mathcal{R}_{\mu\nu}(q) = \delta_{\mu\nu} - 4q_\mu q_\nu/q^2$. A careful study of inclusion of ghost loop in this DSE was performed by [14], and they showed the infrared QCD running coupling in Landau gauge could be finite.

The divergent QCD running coupling caused difficulty in the model building of dynamical chiral symmetry breaking [15, 16]. In order to get reasonable values of the quark condensates, infrared finite QCD running coupling was favored. Recent DSE approach with multiplicative renormalizable(MR) truncation with infrared finite QCD running coupling [17, 18] suggests that the confinement and the chiral symmetry breaking can be explained by the unique running coupling. We thus compare the running coupling obtained from our lattice simulation and that used in the DSE and study the dependence on the Gribov copy.

We produced SU(3) gauge configurations by using the heat-bath method, performed gauge fixing and analyzed lattice Landau gauge configurations of $\beta = 6.4, 56^4$. The $\beta = 6.4, 48^4$ and 56^4 lattices allow measuring the ghost propagator in the momentum range $[0.48, 14.6]$ GeV, and $[0.41, 14.6]$ GeV, respectively. In the present work, the gauge field is defined from the link variables as $\log U$ type:

$$U_{x,\mu} = e^{A_{x,\mu}}, \quad A_{x,\mu}^\dagger = -A_{x,\mu}.$$

The fundamental modular gauge (FMG)[2] of lattice size L is specified by the global minimum along the gauge orbits, i.e.,

$\Lambda_L = \{U | F_U(1) = \text{Min}_g F_U(g)\}$, $\Lambda_L \subset \Omega_L$, where Ω_L is called the Gribov region (local minima) and $\Omega_L = \{U | -\partial D(U) \geq 0, \partial A(U) = 0\}$.

Here $F_U(g)$ is defined as

$$F_U(g) = \|A^g\|^2 = \frac{1}{(n^2 - 1)4V} \sum_{x,\mu} \text{tr} \left(A_{x,\mu}^g A_{x,\mu}^{g\dagger} \right).$$

In the gauge transformation

$$e^{A_{x,\mu}^g} = g_x^\dagger e^{A_{x,\mu}} g_{x+\mu}, \quad (3)$$

where $g = e^{\epsilon \cdot \lambda}$, the value ϵ is chosen depending on the maximum norm $|\partial A|_{cr}$ as follows.

- When $|\partial A| > |\partial A|_{cr}$: $\epsilon_x = \frac{\eta'}{\|\partial A\|} \partial A_x$ ($\eta' \sim 0.05$)
- When $|\partial A| \leq |\partial A|_{cr}$: $\epsilon = (-\partial_\mu D_\mu(A))^{-1} \eta \partial A$ ($\eta \sim 1.6$)

In the second case, calculation of $(-\partial_\mu D_\mu(A))^{-1}$ is performed by Newton's method where the linear equation is solved up to third order of the gauge field, and then the Poisson equation is solved by the multigrid method [19, 20, 21]. The accuracy of the gauge fixed configuration characterized by $\partial A(U) = 0$ is 10^{-4} in the maximum norm which turned out to be about 10^{-15} in the L_2 norm of the gauge field in contrast to about 10^{-12} in 48^4 .

In the calculation of the ghost propagator, i.e. inverse Faddeev-Popov (FP) operator, we adopt the conjugate gradient (CG) method, whose accuracy of the solution in the $q < 0.8$ GeV region turned out to be less than 5% in the maximum norm [5, 7].

In [7], we analyzed these data using a method inspired by the principle of minimal sensitivity (PMS) and/or the effective charge method [22, 23], the contour-improved perturbation method [24] and the DSE approach [10, 14]. We perform the same analysis to the 56^4 data.

The infrared behavior of the running coupling is tightly related to the mechanism of the dynamical chiral symmetry breaking [16, 17, 25]. The lattice data are compared with the theory of dynamical chiral symmetry breaking based on the DSE.

In sec. II we show some details of the gauge fixing procedure and show sample dependence of the gluon propagator, Kugo-Ojima parameter and QCD running coupling. In sec. III a brief summary of the DSE as well as the recent exact renormalization group approach(ERGE) are presented. We compare lattice data with results of the theoretical analysis of DSE. Issues on dynamical chiral symmetry breaking and comparison with the case of SU(2) is discussed in sect IV.

II. GRIBOV COPY AND THE 56^4 LATTICE DATA

The magnitude of $|\partial A|_{cr}$ in the gauge transformation is chosen to be 2.2(copy A) or 2(copy B). In most cases,

gauge fixed configurations are almost the same, but in some cases, different $|\partial A|_{cr}$ produce significantly different copies.

In order to see the difference of the gluon field of the Gribov copies, we measured the 1-dimensional Fourier transform (1-d FT) of the gluon propagator transverse to the lattice coordinate axes. It is equivalent to the specific Schwinger function

$$S(t, \vec{0}) = \frac{1}{\sqrt{L}} \sum_{q_0=0}^{L-1} D_A(q_0, \vec{0}) e^{2\pi i q_0 t/L} \quad (4)$$

where L is the lattice size. Here the function $D_A(q^2)$ is defined as

$$\begin{aligned} D_{A,\mu\nu}(q) &= \frac{1}{n^2 - 1} \sum_{x=\mathbf{x},t} e^{-iqx} \text{Tr} \langle A_\mu(x) A_\nu(0)^\dagger \rangle \\ &= (\delta_{\mu\nu} - \frac{q_\mu q_\nu}{q^2}) D_A(q^2). \end{aligned} \quad (5)$$

When the Schwinger function becomes negative, the reflection positivity becomes violated, which means that the gluon is not a physical particle. Violation of positivity is considered as a sufficient condition of the confinement[10, 25, 26].

The four 1-d FT of the sample I_A and those of the sample I_B are shown in Fig. 1 and in Fig. 2, respectively. The solid line, dotted line, dashed line and the dash-dotted line corresponds to propagator transverse to x_1, x_2, x_3 and x_4 axis in the Euclidean space, respectively.

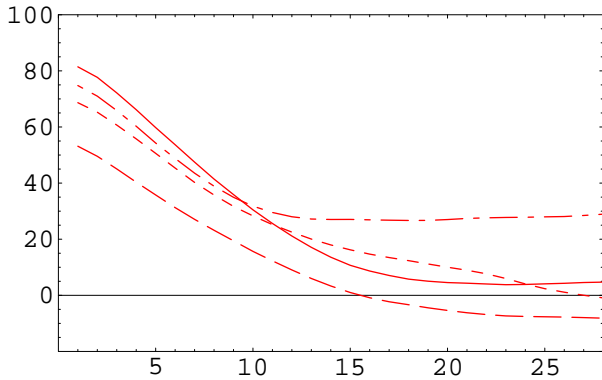


FIG. 1: The 1-d FT of the gluon propagator along the 4 axes. $\beta = 6.4, 56^4$ in the log U definition. sample I_A

We observe that the gluon propagators of sample I_A and I_B have a specific axis along which the propagator manifestly violates reflection positivity. Here, manifestly means that it remains negative in a wide range in the intermediate not only in the large distance in the coordinate space. Propagators along other axes in the sample I_B are shifted from that of I_A and the propagator almost parallel to that manifestly violating reflection positivity remains finite in the sample I_A , but it becomes almost

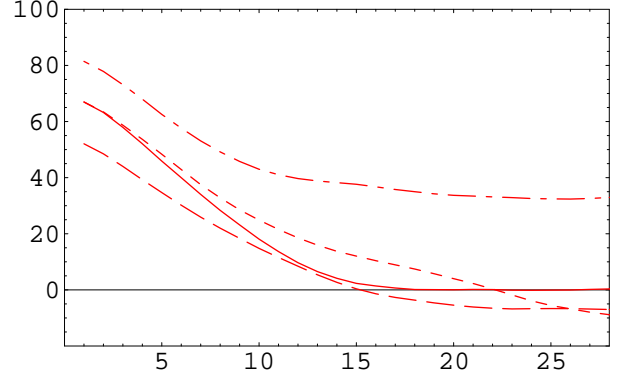


FIG. 2: The 1-d FT of the gluon propagator along the 4 axes. $\beta = 6.4, 56^4$ in the log U definition. sample I_B

0 in the large distance in the sample I_B . The L_2 norm $\|A\|^2$ of sample I_B is smaller than that of I_A .

The ghost propagator is defined by the expectation value of the inverse Faddeev-Popov(FP) operator \mathcal{M}

$$D_G^{ab}(x, y) = \langle \langle \lambda^a x | (\mathcal{M}[U])^{-1} | \lambda^b y \rangle \rangle, \quad (6)$$

via the Fourier transform

$$D_G(q^2) = \frac{G(q^2)}{q^2}. \quad (7)$$

The Kugo-Ojima parameter is defined by the two point function of the covariant derivative of the ghost and the commutator of the antighost and gauge field

$$\begin{aligned} &(\delta_{\mu\nu} - \frac{q_\mu q_\nu}{q^2}) u^{ab}(q^2) \\ &= \frac{1}{V} \sum_{x,y} e^{-ip(x-y)} \langle \text{tr} \left(\lambda^{a\dagger} D_\mu \frac{1}{-\partial D} [A_\nu, \lambda^b] \right)_{xy} \rangle. \end{aligned} \quad (8)$$

We performed the same analyses as sample I for a sample which has the second largest Kugo-Ojima parameter (samples II_A and II_B). The sample dependences of the L_2 norm of the gauge field, Kugo-Ojima parameter $c = -u(0)$, trace divided by the dimension e/d , horizon function deviation parameter h [2, 19] and the infrared exponent of the ghost propagator at 0.4GeV region α_G , are summarized in Table I. An analysis of DSE [34] suggests that 0.4GeV where α_G is measured is not small enough to identify α_G as κ . We expect about a factor 2 difference between α_G and κ .

We observed that in most samples the dependence of the copy on $|\partial A|_{cr}$ is weak as in the case of sample II , and that the large difference of I_A and I_B copies is exceptional. The Table I also shows that α_G , c and h are correlated. In the average of 15 samples of 56^4 lattice data, we incorporate sample A but not B . The α_G of the sample average is 0.22, but that of the I_A copy is 0.27. The I_A copy has a larger L_2 norm of the gauge field but smaller h and larger c . We find that not all samples have the axis that manifestly violates reflection positivity and that the direction of the axis is sample dependent.

A. Kugo-Ojima parameter

Our sample average of $c = -u(0)$, e/d , h , α_G and the exponent of the gluon dressing function near zero momentum α_D and near $q = 1.97\text{GeV}$ α'_D are summarized in Table II.

The color off-diagonal, space diagonal part of the Kugo-Ojima parameter c was 0.0001(162) and consistent to 0. The magnitude of the Kugo-Ojima parameter c and exponent of the ghost propagator α_G are tightly correlated and they are also correlated with the violation of the reflection positivity in the gluon propagator. In the I_A copy, reflection positivity is violated along x_3 axis and the average of 33 and 88 components of c along this axis is 0.97(6), consistent with 1.

B. Gluon propagator

The gluon propagator in momentum space was measured by using cylindrical cut method [27], i.e., choosing momenta close to the diagonal direction. In Fig. 3 we show the gluon dressing function of $\beta = 6.4, 56^4$ lattice data together with 48^4 lattice data. The gluon propagators of $24^4, 32^4$ and 48^4 as a function of the physical momentum agree quite well with one another and they can be fitted by the \widetilde{MOM} scheme[7].

$$D_A(q^2) = \frac{Z(q^2, y)|_{y=0.02227}}{q^2} = \frac{Z_A(q^2)}{q^2} \quad (9)$$

in the $q > 0.8$ GeV region. The gluon propagator of 56^4 shows suppression from the 48^4 in $2 < q < 10$ GeV region but fits the perturbative QCD result above 10 GeV.

C. Ghost propagator

The ghost dressing function is defined by the ghost propagator as $G^{ab}(q^2) = q^2 D_G^{ab}(q^2)$. In Fig. 4, $\beta = 6.4, 48^4$, and 56^4 and $\beta = 6.0$ 24^4 and 32^4 lattice data of the ghost propagator are compared with that of the \widetilde{MOM} scheme[7, 28]

$$D_G(q^2) = -\frac{Z_g(q^2, y)|_{y=0.02142}}{q^2} = \frac{G(q^2)}{q^2}. \quad (10)$$

TABLE I: The Gribov copy dependence of the Kugo-Ojima parameter c , trace divided by the dimension e/d , horizon condition deviation parameter h and the exponent α_G .

	I_A	I_B	II_A	II_B	average
$\ A\ ^2$	0.09081	0.09079	0.090698	0.090695	0.09072(7)
c	0.851(77)	0.837(58)	0.835(53)	0.829(56)	0.827(15)
e/d	0.9535	0.9535	0.9535	0.9535	0.954
h	-0.102	-0.117	-0.118	-0.125	-0.127
α_G	0.272	0.241	0.223	0.221	0.223

TABLE II: The Kugo-Ojima parameter c , trace divided by the dimension e/d , horizon function deviation h in the $\log U$ definitions. The exponent of the ghost dressing function near zero momentum α_G , the exponent of the gluon dressing function near zero momentum α_D , near $q = 1.97\text{GeV}$ α'_D in $\log U$ type. $\beta = 6.0$ and 6.4.

β	6.0			6.4			
	L	16	24	32	32	48	56
c	0.628(94)	0.774(76)	0.777(46)	0.700(42)	0.793(61)	0.827(27)	
e/d	0.943(1)	0.944(1)	0.944(1)	0.953(1)	0.954(1)	0.954(1)	
h	-0.32	-0.17	-0.16	-0.25	-0.16	-0.12	
α_G	0.175	0.175	0.174	0.174	0.193	0.223	
α_D		-0.310	-0.375		-0.273	-0.323	
α'_D	0.38	0.314	0.302	0.31	0.288	0.275	

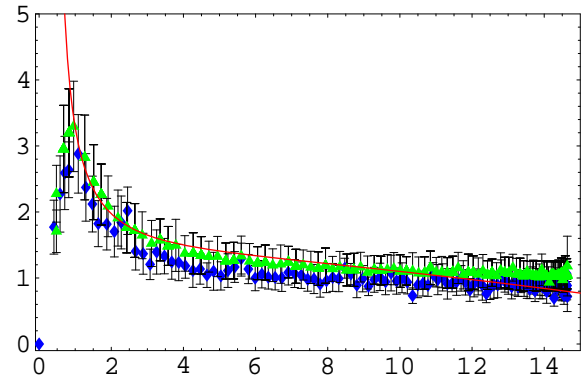


FIG. 3: The gluon dressing function as the function of the momentum $q(\text{GeV})$. $\beta = 6.4, 48^4$ (stars) and 56^4 (diamonds) in the $\log U$ definition. The solid line is that of the \widetilde{MOM} scheme.

We observe that the agreement is good for $q > 0.5$ GeV. The ghost propagator was first measured in [29] but the scaling property was not observed and the lowest momentum point was incorrectly suppressed.

D. QCD running coupling

We measured the running coupling from the product of the gluon dressing function and the ghost dressing function squared [14, 42]. We parametrize infrared power dependence of $D_A(q^2)$ as $\simeq (qa)^{-2(1+\alpha_D)}$ and that of $D_G(q^2)$ as $\simeq (qa)^{-2(1+\alpha_G)}$. Thus,

$$\alpha_s(q^2) = \frac{g_0^2}{4\pi} \frac{Z_A(q^2)G(q^2)^2}{\tilde{Z}_1^2} \simeq (qa)^{-2(\alpha_D+2\alpha_G)}. \quad (11)$$

The lattice size dependences of the exponents α_D and α_G are summarized in Table II.

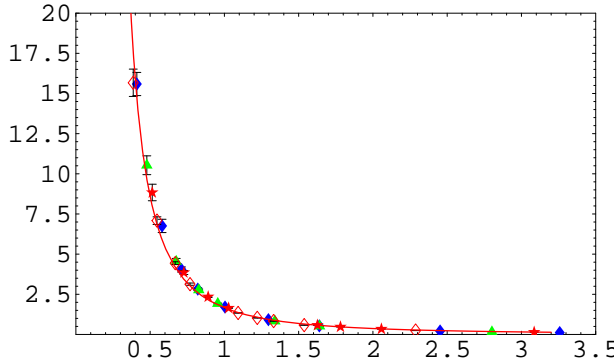


FIG. 4: The ghost propagator as the function of the momentum $q(\text{GeV})$. $\beta = 6.0$, 24^4 (star), 32^4 (unfilled diamond), $\beta = 6.4$, 48^4 (triangle) and 56^4 (filled diamond) in the $\log U$ definition. The fitted line is that of the MOM scheme which is singular at $\tilde{\Lambda}_{\overline{MS}} \simeq 0.35$ GeV.

The vertex renormalization factor \tilde{Z}_1 is 1 in the perturbation theory, but on the lattice it is not necessarily the case. By comparing data of various β , finiteness of \tilde{Z}_1 was confirmed in the case of $SU(2)$ [41]. In the present analysis, we fix \tilde{Z}_1 by normalizing the running coupling by that of the perturbative QCD near the highest momentum point. In the lattice simulation of the three gluon coupling [38], the nonperturbative effect is found to be significant even at 10 GeV region, and a fit of the lattice data by the three loop perturbative term plus c/q^2 correction was proposed. We normalize the running coupling to that of Orsay group at the point of 14.4 GeV, i.e. 0.154(1). This correction revises the previous results of 48^4 lattice data[7] by a factor of 1.97, and the maximum of the running coupling becomes 2.0(3).

In Fig.5 we present the rescaled running coupling of 48^4 lattice and that of the 56^4 lattice and the fit of Orsay group above 2GeV and the result of the MR truncation scheme of Bloch[17, 18], where in addition to the sunset diagram, the squint diagram was included. The running coupling in this DSE is parametrized as

$$\alpha_s(q^2) = \alpha(t\Lambda_{QCD}^2) = \frac{1}{c_0 + t^2} \left(c_0 \alpha_0 + \frac{4\pi}{\beta_0} \left(\frac{1}{\log t} - \frac{1}{t-1} \right) t^2 \right) \quad (12)$$

where $t = q^2/\Lambda_{QCD}^2$. We choose parameter $c_0 = 30$ instead of $c_0 = 15$ [17] and $\alpha_0 = 2.5$ to fit the lattice data.

Phenomenologically fitted Λ_{QCD} from $\alpha(M_Z)$ is about 710 MeV, but the value depends on the number of quark flavors and in the quenched approximation the choice is not appropriate. We choose as [17], $\Lambda_{QCD} = 330$ MeV. The infrared fixed point α_0 is expressed as an analytic function of κ , and [18] claims that when two-loop squint diagrams are included, possible solutions exist only for κ in the range $[0.17, 0.53]$. Our data $\alpha_0 = 2.5$ implies $\kappa \sim 0.5$.

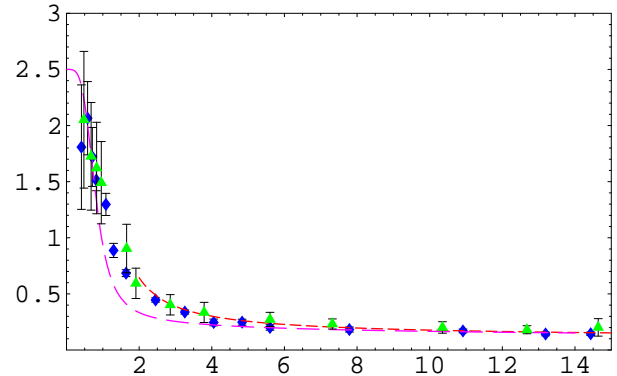


FIG. 5: The running coupling $\alpha_s(q)$ as a function of momentum $q(\text{GeV})$ of the $\beta = 6.4$, 56^4 lattice and 48^4 lattice. The DSE approach with $\alpha_0 = 2.5$ (long dashed line) and the the Orsay group(dotted line) are also plotted.

When the ghost propagator of the exceptional configuration is adopted, suppression of the running coupling at 0 momentum disappears. The DSE results, Orsay fit and the lattice data of the running coupling in which the ghost propagator is taken from the average and taken from that of the I_A copy as a function of logarithm of momentum $\log_{10} q(\text{GeV})$ are shown in Fig.6.

The contour improved perturbation method with $\Lambda = e^{70/6\beta_0} \tilde{\Lambda}_{\overline{MS}}$ in two loop order [7, 24] is consistent with our data at $q > 10\text{GeV}$ region, (dotted line) but in the infrared region it underestimates the lattice data. The dotted line is qualitatively the same as the results of hypothetical τ lepton decay [33].

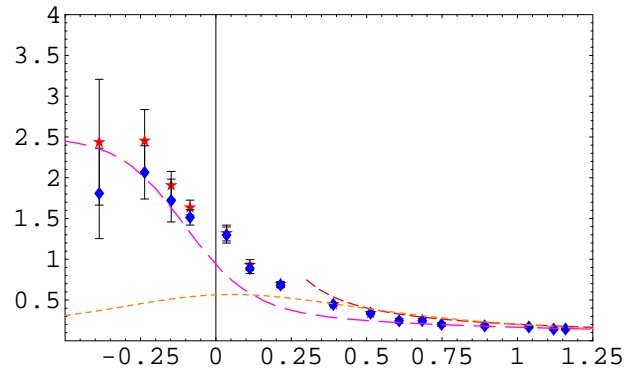


FIG. 6: The running coupling $\alpha_s(q)$ as a function of the logarithm of momentum $\log_{10} q(\text{GeV})$ of the $\beta = 6.4$, 56^4 lattice using the ghost propagator of the I_A copy (star) and that of the average (diamond). The DSE approach with $\alpha_0 = 2.5$ (long dashed line), the fit of the Orsay group perturbative $+c/q^2$ (short dashed line) and the contour improved perturbation method (dotted line) are also shown.

III. COMPARISON WITH DSE AND ERGE

In the DSE approaches, infrared power behavior and specific relation between the exponent of the ghost propagator and the gluon propagator is assumed. In the ERGE, flow equation in terms of the effective average action Γ_Λ where Λ is the infrared cut-off scale is considered[30, 31, 32]. In a recent work four point vertices in addition to the two point vertices are incorporated and the running coupling was calculated via

$$\alpha(q^2) = \frac{g^2(\Lambda_0)}{4\pi f_Z(q^2; \Lambda \rightarrow 0) f_G^2(q^2; \Lambda \rightarrow 0)} \quad (13)$$

where $f_Z(q^2; \Lambda)$ and $f_G(q^2; \Lambda)$ are gluon and ghost propagator function, respectively. They are related to the gluon and ghost propagator as

$$D_{A,\mu\nu}(q^2) = (\delta_{\mu\nu} - q_\mu q_\nu/q^2) \frac{1}{q^2 f_Z(q^2; \Lambda \rightarrow 0)} \quad (14)$$

and

$$D_G(q^2) = -\frac{1}{q^2 f_G(q^2; \Lambda \rightarrow 0)} \quad (15)$$

The infrared exponent κ obtained in this analysis turned out to be $\kappa \sim 0.146$ in contrast to the DSE approach which suggested $\kappa \sim 0.5$. The infrared fixed point $\alpha \sim 4.70$ was predicted which is about factor 2 larger than our lattice simulation.

The prediction $\alpha_0 = 2.6$ and $\kappa = 0.5$ of [18] is consistent with our lattice data. Here we summarize his approach and compare our lattice results.

The quark propagator in Euclidean momentum state is expressed as[17, 25]

$$\frac{1}{-iq_\mu \gamma_\mu A(q^2) + B(q^2)} = \frac{Z(q^2)}{-iq_\mu \gamma_\mu + M(q^2)} \quad (16)$$

and $M(q^2) = B(q^2)/A(q^2)$ is proportional to the quark condensate at large q^2 :

$$M(q^2) \sim m_\mu - \frac{4\pi\alpha_s(q^2)}{3q^2} \left(\frac{\alpha_s(q^2)}{\alpha_s(\mu^2)} \right)^{-d_m} \langle \bar{\psi}\psi(\mu^2) \rangle \quad (17)$$

where $d_m = 12/(33 - 2N_f)$. Here the number of flavor $N_f = 0$ in the quenched approximation.

The quark field is renormalized as

$$Z(q^2, \mu^2) = Z_2(\mu^2, \Lambda^2) Z_R(q^2, \mu^2) \quad (18)$$

where Z_R is the renormalized quark dressing function, Z_2 is the quark field renormalization constant and at the renormalization point. We define $Z_R(x) = Z_R(x, \mu^2)$ and $Z_R(\mu^2) = 1$ and $m_\mu = M(\mu^2)$. In the DSE[18], μ is chosen to be $\Lambda_{QCD} = 330\text{MeV}$.

The renormalized quark dressing function $Z_R(q)$ and the quark mass function $M(q)$ can be calculated by a coupled equation once the running coupling $\alpha_s(q^2)$ is given

[17]. The quark mass function at the origin $M(0)$ is a function of the parameter c_0 and our fitted value $c_0 = 30$ yields

$$M(0) \simeq 1.27\Lambda_{QCD} = 0.419\text{GeV}. \quad (19)$$

This value is consistent with the result of quark propagator in quenched lattice Landau gauge simulation[35] extrapolated to 0 momentum. The quark condensate $\langle \bar{\psi}\psi \rangle$ is estimated as $-(0.70\Lambda_{QCD})^3$ which is compatible with the recent analysis of quenched lattice QCD [36].

IV. DISCUSSION AND OUTLOOK

We measured the gluon dressing function and the ghost dressing function in lattice Landau gauge QCD and calculated the running coupling. In view of uncertainty in the vertex renormalization factor \tilde{Z}_1 which is not necessarily 1 in the lattice simulation, we normalized the running coupling by that of perturbative QCD near the highest momentum point of the lattice simulation. We found infrared fixed point $\alpha_0 \sim 2.5(5)$, which is consistent with the MR scheme DSE calculation [18]. In the momentum dependence, there is disagreement with DSE in $2 < q < 10$ GeV region, which suggests a correction like c/q^2 term in $\alpha_s(q)$ [39]. Although this correction applies only in $q > 2\text{GeV}$ region, it could yield attraction between colored sources.

We observed that the 1-d FT of gluon propagator of the I_A copy has an axis along which the reflection positivity is manifestly violated. The average of Cartan subalgebra components of Kugo-Ojima parameter along this specific axis becomes consistent with $c = 1$. The 1-d FT of the gluon propagator along the diagonal direction in the lattice is also performed by using the analytical expression of the gluon dressing function in \widetilde{MOM} scheme for $q > 1$ GeV and numerical interpolation for $0 < q < 1$ GeV. Since reflection positivity violating axis in the average does not coincide with the diagonal axis, violation of reflection positivity is very weak, although the quantitative feature is sensitive to the dressing function near $q = 0$.

When the QCD running coupling in the infrared region is thought to be divergent, the dynamical chiral symmetry breaking was thought to be irrelevant to confinement[16]. Our lattice data of running coupling is qualitatively similar to that assumed in the model of dynamical chiral symmetry breaking.

In passing, we compare running coupling measured in other lattice simulations. Orsay group measured the running coupling with use of U -linear definition and from triple gluon vertex. The running coupling turned out to behave as $\propto p^4$ in the infrared contrary to ours, but above 0.8 GeV the data are consistent with ours. They analyzed the infrared behavior in the instanton liquid model [38]. Running coupling above 0.2 GeV in instanton scheme was measured by the DESY group [40], and the value in infrared is about factor 1.5 larger than ours.

In the $\beta = 2.2$, 16^4 SU(2) lattice simulation, we normalize the running coupling at the highest momentum point 3.7 GeV by that of the two-loop perturbation method. This correction revises the previous result of the running coupling of SU(2) [7] by about factor 1.54, but there are difference from Tuebingen and São Carlos [42] by about factor 2.

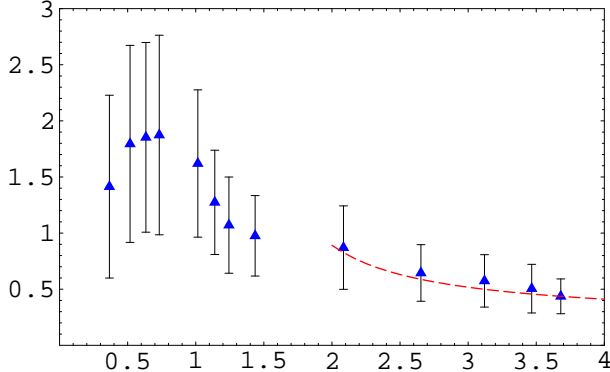


FIG. 7: The SU(2) running coupling $\alpha_s(q)$ as a function of momentum q (GeV) of the $\beta = 2.2$, 16^4 lattice. The result of two-loop perturbation theory (dotted line) are also plotted.

The ghost propagator and the gluon propagator of [42] were rescaled by the tadpole renormalization factor u_P and they cannot be directly compared with our data. There are qualitative agreements in ghost propagator of [42] and ours, but in the gluon propagator there are discrepancies in the momentum dependence in the infrared region. Our gluon propagator below 1 GeV is more suppressed than those of [42]. Since in the running coupling the tadpole renormalization factors u_P cancel [42], the difference in the running coupling $\alpha_s(q)$ in the infrared is due to the difference in the shape of the gluon propagator. We remark that the ghost propagator in U -linear definition becomes larger than that of $\log U$ definition. Its correction in the running coupling is expected to be about 20% in SU(2) [19]. In the case of SU(3), a com-

parison of the ghost propagator in U -linear and $\log U$ definitions of 48^4 lattice suggests larger corrections than in SU(2). Our U -linear gauge fixing of SU(3) is performed on samples which are gauge fixed by using the $\log U$ definition. These differences could explain parts of discrepancies in the running coupling from the DESY data where U -linear definition is adopted.

In the study of instantons, Nahm conjectured that Gribov copies cannot tell much about confinement [4]. We showed that the dynamical chiral symmetry breaking and confinement can be explained by using the same running coupling which has the infrared fixed point $\alpha_0 \simeq 2.5(5)$, and that the Gribov copy gives information on the ambiguity in the parameter that characterizes chiral symmetry breaking and confinement.

We observed that there are samples whose 1-D FT of the gluon propagator transverse to a lattice axis manifestly violates reflection positivity. The direction of the reflection positivity violating axis appears randomly. Recently, Aubin and Ogilvie [43] pointed out that the origin of the reflection positivity violation lies in the quenched character of the gauge transformation g . They demonstrated in a Higgs model type $SU(2)$ 20^4 lattice simulation, occurrence of reflection positivity violation analogous to that in the quenched lattice simulation of a_0 meson propagator, by considering the gauge transformation of $G_{local} \times G_{global}$. Whether these points of view applies to the Landau gauge and whether the population of the exceptional configuration becomes large in larger lattice is to be investigated.

Acknowledgments

We thank the referee for suggesting normalization of the running coupling by that of perturbative QCD in high momentum region. S.F. thanks Kei-Ichi Kondo for attracting our attention to the ERGE approach. This work is supported by the KEK supercomputing project No. 03-94.

[1] V.N. Gribov, Nucl. Phys. **B** **139** (1978).
 [2] D. Zwanziger, Nucl. Phys. **B** **364**, 127 (1991), *ibid* **B** **412**, 657 (1994).
 [3] D. Zwanziger, Phys. Rev. D **69**, 016002 (2004), arXiv:hep-ph/0303028.
 [4] W. Nahm, in *IV Warsaw Symp. on Elem. Part. Phys.* ed. Z. Ajduk, p.275 (Warsaw 1981).
 [5] H. Nakajima and S. Furui, Nucl. Phys. **B** (Proc. Suppl.) **129-130** (2004), arXiv:hep-lat/0309165.
 [6] T. Kugo and I. Ojima, Prog. Theor. Phys. Suppl. **66**, 1 (1979).
 [7] S. Furui and H. Nakajima, Phys. Rev. D **69**, 074505 (2004), arXiv:hep-lat/0305010.
 [8] A. Cucchieri, Nucl. Phys. **B521**, 365 (1998), arXiv:hep-lat/9711024.
 [9] C.D. Roberts and A. Williams, Prog. Part. Nucl. Phys. **33**, 477 (1994), arXiv:hep-ph/9403224.
 [10] R. Alkofer and L. von Smekal, Phys. Rep. **353**, 281 (2001), arXiv:hep-ph/0007355.
 [11] K-I. Kondo, arXiv:hep-th/0303251.
 [12] S. Mandelstam, Phys. Rev. D **20**, 3223 (1979).
 [13] N. Brown and M.R. Pennington, Phys. Rev. D **39**, 2723 (1989).
 [14] L. von Smekal, A. Hauck, R. Alkofer, Ann. Phys. (N.Y.) **267**, 1 (1998), arXiv:hep-ph/9707327;
 [15] H. Pagels, Phys. Rev. D **19**, 3080 (1979).
 [16] K. Higashijima, Phys. Rev. D **29**, 1228 (1984).
 [17] J.C.R. Bloch, Phys. Rev. D **66**, 034032 (2002), arXiv:hep-ph/0106055.

ph/0202073;

[18] J.C.R. Bloch, Few Body Syst **33**,111(2003).

[19] H.Nakajima and S. Furui, Nucl. Phys. **B** (Proc Suppl.)**63A-C**,635, 865(1999), Nucl. Phys. **B** (Proc Suppl.)**83-84**,521 (2000), **119**,730(2003); Nucl. Phys. **A** **680**,151c(2000), arXiv:hep-lat/0006002, 0007001, 0208074.

[20] S. Furui and H. Nakajima, in *Quark Confinement and the Hadron Spectrum IV*, Ed. W. Lucha and K.M. Maung, World Scientific, Singapore, p.275(2002), hep-lat/0012017.

[21] H. Nakajima and S. Furui, in *Strong Coupling Gauge Theories and Effective Field Theories*, Ed. M. Harada, Y. Kikukawa and K. Yamawaki, World Scientific, Singapore, p.67(2003), arXiv:hep-lat/0303024.

[22] P.M.Stevenson, Phys. Rev. **D23**, 2916(1981);

[23] G. Grunberg, Phys. Rev. **D29**, 2315(1984);

[24] D.M. Howe and C.J. Maxwell, arXiv:hep-ph/0204036 v2.

[25] C.S. Fischer and R. Alkofer, Phys. Rev. **D67**,094020(2003).

[26] M. Stingl, Phys. Rev. **D34**,3863(1986),Z. Phys. **A353**,423(1996).

[27] D.B. Leinweber, J.I. Skullerud, A.G. Williams and C. Parrinello, Phys. Rev. **D60**,094507(1999); ibid Phys. Rev. **D61**,079901(2000).

[28] K. Van Acoleyen and H. Verschelde, Phys. Rev. **D66**,125012(2002),arXiv:hep-ph/0203211.

[29] H. Suman and K. Schilling, Phys. Lett. B **373**,314 (1996)

[30] C. Wetterich, Phys. Lett. B**301**,90(1993).

[31] U. Ellwanger, M. Hirsch and A. Weber, Eur. Phys. J. C1, 563(1998).

[32] J. Kato, arXiv:hep-th/0401068.

[33] S.J. Brodsky, S. Menke and C. Merino, Phys. Rev. **D67**,055008(2003), arXiv:hep-ph/0212078 v3.

[34] C.S. Fischer, R. Alkofer and H. Reinhardt, arXiv:hep-ph/0202195.

[35] F.D.R.Bonnet, P.O.Bowman, D.B.Leinweber, A.G.Williams and J.B.Zhang, Phys. Rev. **D65**,114503(2002).

[36] D.Bećirević and V. Lubicz, arXiv:hep-ph/0403044

[37] Ph. Boucaud et al., Phys. Rev. **D61**,114508(2000), arXiv:hep-ph/9910204.

[38] Ph. Boucaud et al., arXiv:hep-ph/0212192.

[39] Ph. Boucaud el al., arXiv:hep-ph/0003020 v2.

[40] A. Ringwald and F. Schrempp, Phys. Lett. B **459**,249(1999), arXiv:hep-lat/9903039.

[41] J.R.C.Bloch, A. Cucchieri, K.Langfeld and T.Mendes, Nucl. Phys. **B**(Proc. Suppl.)**119**,736 (2003); arXiv:hep-lat/0209040 v2.

[42] J.C. Bloch, A. Cucchieri, K. Langfeld and T. Mendes, Nucl. Phys. **B** **687**,76(2004); arXiv:hep-lat/0312036 v1.

[43] C. Aubin and M.C. Ogilvie, hep-lat/0406014 v1.